2017-10-31

# Compact electronic system for complex impedance measurement and its experimental verification

Simić Mitar, Goran Stojanović

2017 European Conference on Circuit Theory and Design (ECCTD)

# Compact Electronic System for Complex Impedance Measurement and its Experimental Verification

Mitar Simić
University of Banja Luka
Faculty of Electrical Engineering
Banja Luka, Bosnia and Herzegovina
mitar.simic@etf.unibl.org

Goran M. Stojanović
University of Novi Sad
Faculty of Technical Sciences
Novi Sad, Serbia
sgoran@uns.ac.rs

***Abstract*—Electrical impedance measurement is very important in characterization process of sensors and new materials. In laboratory measurements use of commercial impedance analyzers is often as such devices offer high measurement accuracy and reliability. However, development of measurement devices for *in-situ* measurements is very important, because of limitations of impedance analyzers related to the dimensions, complexity and price. In this paper, we present theoretical background for design and development of portable and compact electronic device for complex impedance measurement. Our approach consists of generation of the reference AC voltage, which will cause flow of electrical current through the device under test (DUT), and processing of the voltage across of the DUT with Discrete Fourier Transformation (DFT). Hardware prototype of the measurement system based on the proposed approach has been developed. Experimental verification and comparison with commercial impedance measurement systems determined the measurement accuracy of the developed device.**

***Keywords—DFT, impedance measurement, window functions.***

## I. Introduction

Impedance measurement is very important part of sensors and materials characterization [1]. For laboratory measurements it is common to use commercial impedance analyzers. Commercial impedance analyzers usually have very high accuracy, wide frequency and measurement ranges as well as different test modes. However, big dimensions, need for grid supply and high price are also very common.

However, for the sensor applications in real environmental conditions (*in-situ* measurements) it is required to perform impedance measurements outside the laboratory. Need for the portable impedance measurement devices is emphasized with current trends of remote environmental monitoring with various impedimetric sensors [2, 3], portable bioimpedance measurement applications [4], impedance spectroscopy testing of anticorrosion coatings on steel structures [5], etc. Measurement devices for such applications should be designed to meet specific requirements of that application regarding measurement and frequency range. This can simplify structure of the measurement device because, in many cases, there is no need for wide frequency and measurement ranges. Such approach can lead to impedance measurement devices with low complexity and small dimensions. Consequently, it is expected that measurement device will be low cost. However, relatively high accuracy and reliability are still required.

There are many measurement methods to choose from when measuring impedance, each of which has advantages and disadvantages. Some of the measurement principles are: bridge method, auto-balancing bridge method, resonant method, and I-V method [6]. However, main disadvantage of the bridge method is a need to be manually balanced and limitation that it can be used in very narrow frequency range. With auto-balancing bridge method, higher frequency ranges are not available. For the resonant method, circuit has to be tuned to the resonance and generally it leads to low impedance accuracy. I-V method usually use low loss transformer, which limits the low end of the applicable frequency range. Reported issues [6] give a strong motivation for the development of the measurement techniques suitable for implementation in low cost portable measurement systems.

This work presents design and prototyping of impedance measurement system suitable for low cost and portable devices. Our approach consists of generation of the reference AC voltage, which will cause flow of electrical current through the DUT, and processing of the voltage across of the DUT with DFT. We have developed hardware prototype of the measurement system based on the proposed approach. Experimental verification and comparison with commercial impedance measurement systems determined the measurement accuracy of the developed device.

## II. Methods

### A. Theoretical overview of the proposed method

Block scheme of our proposed impedance measurement system is presented in Fig. 1.

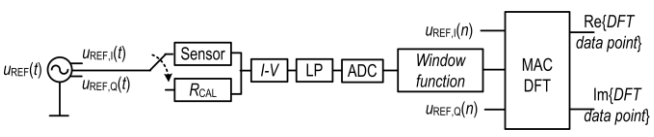


Fig. 1. Block scheme of the proposed approach.

AC voltage generator, which generates the referent harmonic excitation, $u_{REF}(t)$, is connected to the one connection point of the calibration resistor ($R_{CAL}$) or DUT. Second connection points of the $R_{CAL}$ and DUT are connected to the ground or to some DC bias. Thus, there will be electrical current flowing through connected impedance. Following part is current to voltage (I-V) converter which converts value of the electrical current which flowing through the DUT to the equivalent value of the voltage (with defined gain). That voltage is then filtered and sampled with low pass (LP) filter and analog to digital converter (ADC), respectively. Next step is windowing of the discretized signal. After multiplication with window function, samples of the output discrete voltage are then multiplied with samples which are *in-phase* ($u_{REF,I}(n)$) and *in-quadrature* ($u_{REF,Q}(n)$) with samples of the AC reference voltage ($u_{REF}(n)$). Multiply and accumulate operations are done with DFT MAC block. Outputs are real (Re{$X(f)$}) and imaginary (Im{$X(f)$}) part of the DFT data point $X(f)$ at the frequency $f$.

### B. Reference AC voltage generation

To achieve generation of the voltage in a wide frequency range, direct digital synthesizer (DDS) method has been used. Block schematic of DDS is presented in Fig. 2. DDS consists of the reference oscillator, numerically controlled oscillator, frequency control register, digital-to-analog convertor (DAC) and post-filter.

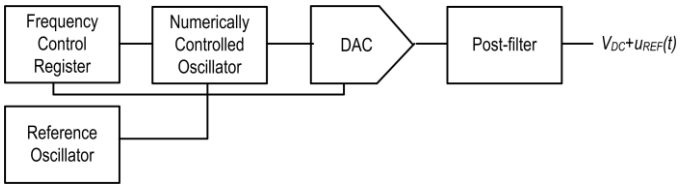


Fig. 2. Block scheme of the DDS.

### C. Current to voltage converter

The basic structure of the current to voltage converter is presented in Fig. 3. To achieve DC-free voltage on the DUT, one input the operational amplifier is biased with $V_{DD}/2$.

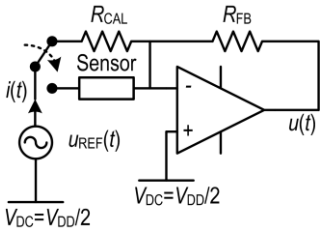


Fig. 3. Basic structure of the current to voltage converter.

If the reference voltage $u_{REF}(t)$ can be presented as $u_{REF}(t)=U_{REF}\sin\omega t$, electrical current flowing through calibration resistor or DUT is defined with:

$$i(t) = \frac{U_{REF}}{Z}\sin(\omega t - \varphi) \qquad (2.1)$$

where $Z$ is magnitude and $\varphi$ is phase angle of the analyzed impedance. Therefore, output voltage $u(t)$ is:

$$u(t) = \frac{V_{DD}}{2} - R_{FB}\frac{U_{REF}}{Z}\sin(\omega t - \varphi) \qquad (2.2).$$

Resistor $R_{FB}$ represents feedback resistor for current to voltage gain tuning. Value of the resistance of this resistor is very important in aim to prevent saturation of the AD converter in the following block. If the DC bias was set to $V_{DD}/2$, then the amplitude of the AC voltage has to be equal or lower than $V_{DD}/2$. Thus, value of the resistance of the $R_{FB}$ resistor which will keep AD converter out of saturation is:

$$R_{FB} = \frac{V_{DD}}{2}\frac{Z_{MIN}}{U_{REF}} \qquad (2.3)$$

where $Z_{MIN}$ is the minimum impedance magnitude of the DUT and $U_{REF}$ is amplitude of the reference AC voltage.

In our approach, to ensure wide impedance measurement range, variable value for calibration and feedback resistors was proposed by use of the analog switches connected with high accuracy resistor networks (0.1% tolerance).

### D. Data acquisition and processing block

Output signal of the current to voltage conversion block is filtered with the low pass filter and connected to the input of the ADC, as shown in Fig. 4.

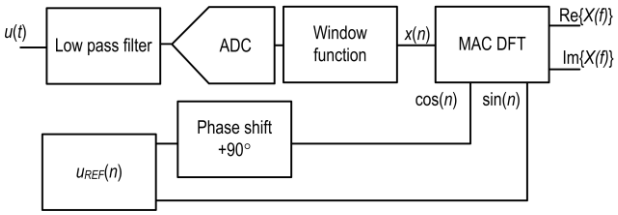


Fig. 4. Structure of the receive stage block.

Because of the data processing, after ADC it is required to limit signal duration in time. This is usually done with windowing (multiplication with window function). In digital signal processing, there are many window function such as rectangular, Bartlett, Hamming, Hann and Blackman [7]. Main parameters of the window functions are Main Lobe Width (MLW), Relative Side Lobe Attenuation (RSLA) and Leakage Factor (LF). More detailed theoretical analysis, provides the optimal values for these parameters: low MLW, high RSLA and low LF [7]. In practice, these requirements are contradictory. Window functions with high RSLA usually have very high LF. Thus, it is necessary to made a compromise when choosing window function. In our research, the use of the Hann window function is proposed as it offers low level computation complexity and good performances [7]. Moreover, there is a smooth transition from non-zero to zero values which leads to very good RSLA. Hann window function is also known as "raised cosine" window. It is described with following expression:

$$W_H(n) = 0.5\left(1 - \cos\frac{2n\pi}{N}\right) \qquad (2.4)$$

for $n$=0,1,..,$N$-1.

After multiplication with the window function, output samples ($x(n)$) are passed to MAC DFT block. MAC DFT block performs multiplication with *in-phase* and *in-quadrature* samples, and accumulation in 1024 points (proposed DFT resolution), at each test frequency $f$. After this operation, the output is real and imaginary part of the DFT data point:

$$X(f)=\sum_{n=0}^{1023}x(n)[\cos(n)-j\sin(n)]=\mathrm{Re}\{X(f)\}+j\,\mathrm{Im}\{X(f)\} \quad (2.5)$$

This value does not represent impedance magnitude, because it has to been multiplied with Gain Factor ($GF$). $GF$ can be determined in calibration process with resistor with known resistance ($R_{CAL}$). Obtained value for $M(f)$ with calibration resistor is then used with $R_{CAL}$ value for $GF$ calculation:

$$GF(f)=\frac{1}{R_{CAL}M(f)} \quad (2.6)$$

which is then used for impedance magnitude calculation of the DUT:

$$Z(f)=\frac{1}{GF(f)M(f)} \quad (2.7)$$

Phase angle of the DFT data point can be calculated as:

$$\Phi(f)=\tan^{-1}\frac{\mathrm{Im}\{X(f)\}}{\mathrm{Re}\{X(f)\}} \quad (2.8)$$

Similarly to impedance magnitude, for determination of the phase angle of the DUT, it is required to calculate phase shift induced by the measurement system itself, $\Phi_S(f)$, and to subtract it from $\Phi(f)$. $\Phi_S(f)$ can be determined in calibration process with $R_{CAL}$ resistor because in that case there is no phase shift induced by the DUT.

## III. Experimental – Hardware Outcome

Main aim in realization of the measurement system was to develop a low cost device with small dimensions and high level of integration with different measurement and data acquisition systems. Because of that, high quality integrated circuits were used: integrated circuit AD5933 for reference voltage generation and signal processing, microcontroller ATmega128 and operational amplifier AD8606 for realization of the current to voltage converter.

Developed impedance measurement system is proposed for use in frequency sweep operation in range of 5 kHz to 100 kHz. Moreover, the developed system can be battery powered (with typical power consumption of 700 mW), in case that portable and autonomous operation is needed for *in-situ* measurements. Amplitude of the output AC voltage can be selected as one from four options: 100 mV, 200 mV, 500 mV or 1000 mV. The system includes a thin film transistor (TFT) display, an embedded keypad, an SD card for local data storage. The device has self-calibration system and implemented algorithm for auto-ranging in impedance measurement. Thus, no additional components nor manual range switching are required during the measurement, which ensures rapid and automated operation. Analog front electronics for signal conditioning was developed in such a way that the presented system operates in two-electrode mode. Hardware outcome of the measurement system is presented in Fig. 5.

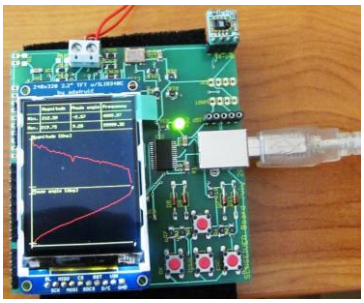

Fig. 5. Hardware outcome of the measurement system.

## IV. Results and Discussion

Accuracy tests of the developed measurement device were done with capacitor $C$=470 pF, series and parallel RC circuit ($R$=390 Ω, $C$=4.7 nF). Agilent 4263B LCR meter was used as a reference measurement device at frequencies of 10 kHz and 100 kHz, while with developed device frequency sweep (1900 Hz frequency step) was performed in a frequency range from 5 kHz to 100 kHz. Obtained results are presented in Fig. 6-8 and Tables I-III.

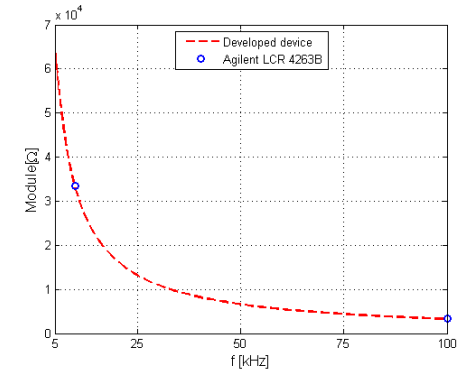


(a)

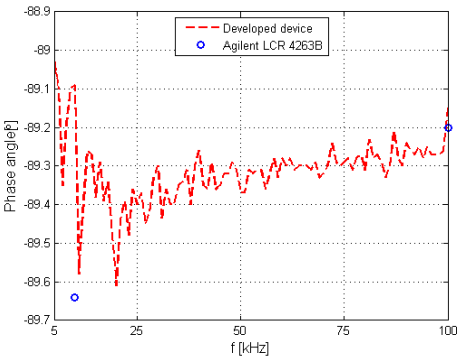


(b)

Fig. 6. Comparison of impedance measurements of a capacitor: (a) module and (b) phase angle.

TABLE I. Comparison of Measurements for a Capacitor.

| | Agilent 4263B | Developed device | Error | $f$ [kHz] |
|---|---|---|---|---|
| $Z$ | 33336.0 Ω | 32735.7 Ω | 1.89% | 10 |
| $\varphi$ | -89.64° | -89.09° | 0.55° | 10 |
| $Z$ | 3359.8 Ω | 3260.82 Ω | 2.95 | 100 |
| $\varphi$ | -89.2° | -89.15° | 0.05° | 100 |

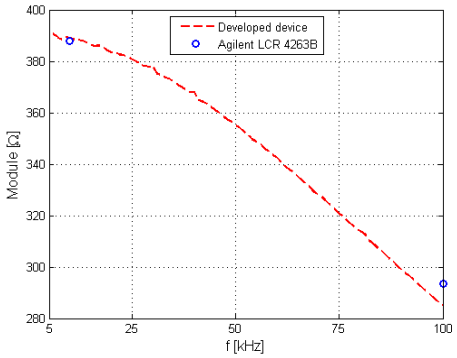


(a)

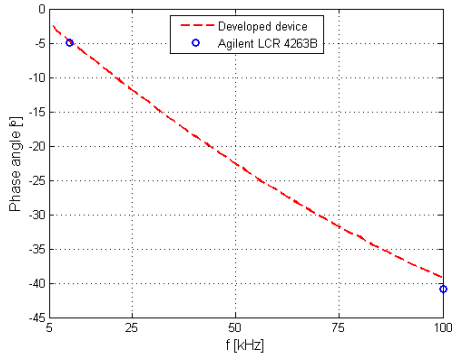


(b)

Fig. 7. Comparison of impedance measurements of parallel RC circuit: (a) module and (b) phase angle.

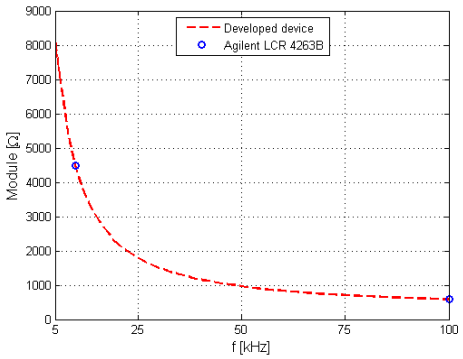


(a)

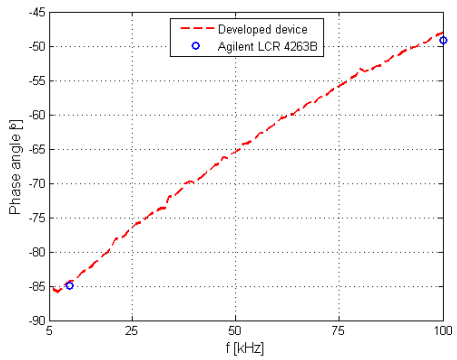


(b)

Fig. 8. Comparison of impedance measurements of series RC circuit: (a) module and (b) phase angle.

TABLE II. COMPARISON OF MEASUREMENTS FOR PARALLEL RC CIRCUIT.

| | **Agilent 4263B** | **Developed device** | **Error** | ***f* [kHz]** |
|---|---|---|---|---|
| ***Z*** | 387.82 Ω | 389.06 Ω | 0.32% | 10 |
| ***φ*** | -4.96° | -4.71° | 0.25° | 10 |
| ***Z*** | 293.5 Ω | 284.89 Ω | 2.93% | 100 |
| ***φ*** | -40.92° | -39.22° | 1.7° | 100 |

TABLE III. COMPARISON OF MEASUREMENTS FOR SERIES RC CIRCUIT.

| | **Agilent 4263B** | **Developed device** | **Error** | ***f* [kHz]** |
|---|---|---|---|---|
| ***Z*** | 4492.1 Ω | 4417.44 Ω | 0.32% | 10 |
| ***φ*** | -84.89° | -84.28° | 0.61° | 10 |
| ***Z*** | 596.11 Ω | 586.68 Ω | 1.56% | 100 |
| ***φ*** | -49.18° | -48.0° | 1.18° | 100 |

Detailed analysis of obtained results determined measurement accuracy of the developed device to 3% in measurements of impedance module and 2° for phase angle, which is suitable for the most practical applications. Moreover, main characteristics of the developed device regarding dimensions (7.7x7.5 $cm^2$) and modularity make it very suitable for portable applications.

## V. CONCLUSION

In this paper a description of the system for the *in-situ* impedance measurement has been given. Our approach eliminates issues related to the measurement accuracy and complexity of commonly used measurement methods, and offers measurement accuracy acceptable for the most practical applications. Main purpose of developed device is environmental sensors characterization, bioimpedance measurements and testing of materials properties.

## ACKNOWLEDGMENT

Authors would like to thank EC for support within the project MEDLEM no. 690876 as well as Prov. Secr. for higher education no. 114-451-2072/2016.

## REFERENCES

[1] N. Bananos, B. C. H Steele, and E. P. Butler, “Characterization of the materials” in Imedance Spectroscopy: Theroy, Experiment, and Applications, Second edition, E. Barsoukov, and J. R. Macdonald, Eds. Willey Interscience, 1987, pp. 205-263.

[2] M. Simić, L. Manjakkal, K. Zaraska, G. M. Stojanović, and R. Dahiya, "$TiO_2$ based thick film pH sensor", *IEEE Sensors Journal*, Vol. 17, No. 2, pp. 248-255, 2017.

[3] L. Manjakkal, E. Djurdjic, K. Cvejin, J. Kulawik, K. Zaraska, and D. Szwagierczak, “Electrochemical impedance spectroscopic analysis of $RuO_2$ based metal oxide thick film pH sensors,” *Electrochim. Acta*, vol. 168, pp. 246–255, 2015.

[4] L. Beckman, D. Riesen, and S. Leonhardt, "Optimal electrode placement and frequency range selection for the detection of lung water using bioimpedance spectroscopy", In *Proc. 29th IEEE EMBS*, Aug. 2007, pp. 2685-2688.

[5] J. Hoja, and G. Lentka, "Portable analyzer for impedance Spectroscopy", In *Proc. XIX IMEKO*, Sept. 2009, 497-502.

[6] Agilent Impedance Measurement Handbook: A guide to measurement technology and techniques, 4th Ed., Agilent Technologies, Inc., 2013.

[7] P. Podder, T. Z. Khan, M. H. Khan, and M. M. Rahman, "Comparative performance analysis of Hamming, Hanning and Blackman window," *International Journal of Computer Applications*, vol. 96, no. 18, 2014.